THE JOURNAL OF BIOLOGICAL CHEMISTRY
Vol. 278, No. 50, Issue of December 12, pp. 50234–50239, 2003
Printed in U.S.A.

Separate Roles for the Golgi Apparatus and Lysosomes in the Sequestration of Drugs in the Multidrug-resistant Human Leukemic Cell Line HL-60*

Received for publication, June 23, 2003, and in revised form, September 2, 2003
Published, JBC Papers in Press, September 30, 2003, DOI 10.1074/jbc.M306606200

Yuping Gong, Muralikrishna Duvvuri, and Jeffrey P. Krise‡

From the Division of Drug Delivery and Disposition, School of Pharmacy, University of North Carolina at Chapel Hill, Chapel Hill, North Carolina 27599

The sequestration of drugs away from cellular target sites into cytoplasmic organelles of multidrug-resistant (MDR) cancer cells has been recently shown to be a cause for ineffective drug therapy. This process is poorly understood despite the fact that it has been observed in a large number of MDR cancer cell lines. Analysis of drug sequestration in these cells has traditionally been done using fluorescent anthracycline antibiotics (*i.e.* daunorubicin, doxorubicin). This narrow selection of substrates has resulted in a limited understanding of sequestration mechanisms and the intracellular compartments that are involved. To better characterize this phenotype, we chose to examine the sequestration of molecules having different acid/base properties in the MDR HL-60 human leukemic cell line. Here we show that weakly basic drug daunorubicin is sequestered into lysosomes according to a pH partitioning type mechanism, whereas sulforhodamime 101, a zwitterionic molecule, is sequestered into the Golgi apparatus through a drug transporter-mediated process. Quantitative intracellular pH measurements reveal that the lysosome-to-cytosol pH gradient is expanded in the MDR line. Moreover, the MDR cells overexpress the multidrug resistance-related protein (MRP1), which is localized to the Golgi apparatus. These results demonstrate, for the first time, that two distinct mechanisms for intracellular compartmentalization are operational in a single MDR cell line.

The resistance of tumor cells to anticancer agents remains a major cause of treatment failure in patients with cancer. MDR[1] is a term used to describe a resistance phenotype in which cells become simultaneously resistant to different drugs with no obvious structural similarities or mechanisms of action (1). The emergence of MDR is multifactorial. Decreased drug accumulation and/or increased efflux, increased detoxification, increased DNA repair, and altered cell cycle regulation have all been implicated (2). Interestingly, many MDR cell lines have demonstrated the capacity to compartmentalize drugs away from intracellular target sites (3). In drug-sensitive cell lines, chemotherapeutic agents are localized to a significant extent within the cell nucleus. In contrast, the MDR cells compartmentalize drug within distinct cytoplasmic organelles. This sequestration serves to protect the MDR cell from the cytotoxic effects of drugs since cellular targets are often associated with the nucleus.

There are at least two mechanistic explanations that can be used to rationalize the exaggerated drug sequestration capacity of subcellular compartments contained within MDR cancer cells (3). The first involves members of the ATP binding cassette superfamily of transporter proteins such as P-glycoprotein (P-gp) and the multidrug resistance-related protein 1 (MRP1). The overexpression of these transporter proteins in MDR cell lines is well known, and they are traditionally thought to participate in drug efflux at the plasma membrane (4). Recent evidence suggests that these transporters may also drive sequestration into organelles (5).

Immunofluorescence studies have demonstrated that a number of different ATP binding cassette transporters are localized to intracellular compartments in MDR cell lines (6–11). However, some controversy exists as to whether or not the observed intracellular localization of these proteins is a normal component of their biosynthesis, processing, and transport from the endoplasmic reticulum to the plasma membrane. Nevertheless, when these proteins are expressed at the plasma membrane, they have been shown to be involved in the transport of a wide range of substrates including weakly acidic, neutral, and basic compounds (12).

For weakly basic drugs, the accumulation in sequestering organelles can be explained by alterations in intracellular pH gradients. The lumenal pH of lysosomes has been shown to be considerably lower in MDR cells, resulting in an enhanced lysosome-to-cytosol pH differential (3, 13). This can provide a driving force for the accumulation of weakly basic compounds into acidic organelles (2, 14–16). This phenomenon also occurs in normal non-transformed cells and is referred to as lysosomotropism (17). Lysosomotropic agents are characteristically defined as weak bases with pK_a near 7 and are membrane-permeable in the non-ionized form but relatively impermeable in the ionized form. At cytoplasmic pH (pH ~7.2), a significant fraction of these molecules will exist in the non-ionized form and will readily permeate lipid bilayers of subcellular organelles. When these drugs diffuse into acidic compartments such as lysosomes (pH 4–5), they become ionized to a greater extent and less able to diffuse back through the lipid bilayer. In transformation from a normal cell to a cancerous one, it has been shown that the lumenal pH of lysosomes from the cancer

* The costs of publication of this article were defrayed in part by the payment of page charges. This article must therefore be hereby marked "*advertisement*" in accordance with 18 U.S.C. Section 1734 solely to indicate this fact.

‡ To whom correspondence should be addressed. Tel.: 919-843-2277; Fax: 919-966-0197; E-mail: krise@unc.edu.

[1] The abbreviations used are: MDR, multidrug-resistant; BSO, buthionine sulfoximine; FITC, fluorescein isothiocyanate; PBS, phosphate-buffered saline; TRITC, tetramethylrhodamine isothiocyanate; NBD, 12-(*N*-methyl-*N*-(7-nitrobenz-2-oxa-1,3-diazol-4-yl)); C6-ceramide, *N*-hexanoylsphingosine; SNARF1 AM, seminaphthorhodafluor acetoxymethylester; HPLC, high pressure liquid chromatography; MTT, 3-(4,5-dimethylthiazol-2-yl)-2,5-diphenyltetrazolium bromide; SR101, sulforhodamime 101; V-ATPase, vacuolar (H^+)-ATPases; P-gp, P-glycoprotein.

cell is elevated by at least 1.5 pH units (16). Consequently, the pH differential between the lysosomes and the cell cytosol is reduced. This, in turn, results in decreased sequestration of these compounds into the lysosomal compartment. In MDR cancer cells, lysosomal acidification is thought to be re-established (18). Thus, the lysosome-to-cytosol pH differential is again expanded, which in turn provides the driving force for the accumulation of weakly basic drugs. In summary, both normal cells and MDR cancer cells have acidic lysosomes, which can result in weak base sequestration. Alternatively, drug-sensitive cancer cells have a significantly reduced sequestration capacity due to the less acidic nature of their lysosomal compartment.

Previous reports on this topic have proposed either the involvement of drug transporters or the involvement of a pH partitioning type mechanism, but never both. We describe experiments here that show, for the first time, that both of these mechanisms are simultaneously operational in the MDR HL-60 human leukemic cell line. Daunorubicin, a weakly basic anticancer drug, is sequestered into the lysosomal compartment via a pH partitioning mechanism. The zwitterionic molecule, sulforhodamine 101 (SR101), is sequestered into the Golgi apparatus through an MRP1-mediated pathway.

EXPERIMENTAL PROCEDURES

The human acute promyeloid leukemia cell line HL-60 and its doxorubicin-selected resistant HL-60 ADR cell line were kindly provided by Dr. Yueshang Zhang (Arizona Cancer Center, University of Arizona). Cell lines were grown in RPMI 1640 medium supplemented with 10% fetal calf serum, 10 mM Hepes, 1 mM sodium pyruvate, 0.1% penicillin, 0.1% streptomycin. Cells were maintained at a density of 1×10^5 to 1×10^6 cells/ml at 37 °C in a humidified 5% CO_2 atmosphere. Daunorubicin, MK571, nigericin, monensin, concanamycin A, buthionine sulfoximine (BSO) were purchased from Sigma. Sulforhodamine 101, NBD-C_6-ceramide, FITC-dextran (molecular weight, 10,000), (5-and 6-) carboxyl SNARF1 AM acetate ester, Lysotracker Green DND-26, and Oregon Green were obtained from Molecular Probes (Eugene, OR).

Fluorescence Co-localization Experiments—Cells were grown to a density of 1×10^6 cells/ml prior to experimentation. Lysotracker Green or FITC-dextran was used to stain lysosomes. Lysotracker Green (100 nM) was incubated with cells for 1 h at 37 °C. FITC-dextran (5 mg/ml) was incubated with cells for 30 min, which was followed by a 24-h incubation in medium devoid of the dextran. To label the Golgi apparatus, cells were incubated with NBD-C_6-ceramidine (5 μM) for 30 min. Following incubation with probe/drug, cells were pelleted (1,000 rpm, 5 min) and washed twice with ice-cold PBS to remove unincorporated compounds. Cells were viewed with a microscope (Leica Diaplan, Leitz Weltzar, Germany) equipped for epifluorescence with a ×100 objective, and images were captured using an Orca ER camera (Hamamatsu Corp.) controlled by SimplePCI imaging software (Compix Inc.). The data were exported as 8-bit TIFF files and processed using Adobe PhotoShop.

Immunofluorescence—Cells were fixed using 3.7% formaldehyde for 30 min at room temperature. Cells were permeabilized and blocked using 0.05% saponin, 5% goat serum in PBS for 30 min. Primary and secondary antibody incubations were in PBS containing 5% goat serum and 0.05% saponin for 1 h. The primary rat monoclonal antibody for MRP1 (MRPr1, Monosan Antibodies, Uden, The Netherlands) and the primary mouse monoclonal antibodies to the trans-Golgi network-specific protein p230 and the lysosomal membrane protein LAMP-1 (BD Transduction Laboratories) were all diluted 1:100. Following primary antibody incubations, cells were washed four times with PBS containing 0.05% saponin. Secondary antibodies (FITC-labeled goat anti-rat and TRITC-labeled goat anti-mouse, both from Sigma) were diluted 1:500. Cells were subsequently washed four times with PBS prior to fluorescence microscopy.

Protein Expression in Cell Membranes—A post-nuclear supernatant was prepared from 50×10^6 cells pelleted at 1000 rpm for 5 min and washed twice with ice-cold PBS. The cell pellet was suspended in 1 ml of hypotonic buffer containing 15 mM potassium chloride, 1.5 mM magnesium acetate, 1 mM dithiothreitol, and 10 mM Hepes (pH 7.4) supplemented with 0.1 mM phenylmethylsulfonyl fluoride, 5 mg of DNase I, and 1 μg/ml each of aprotin, leupeptin, and pepstatin. Cells were allowed to swell on ice for 10 min followed by 20 strokes with a Dounce homogenizer (pestle B). Subsequently, 0.2 ml of a solution containing 375 mM potassium chloride, 22.5 mM magnesium acetate, 1 mM dithiothreitol, and 220 mM Hepes at pH 7.4 was added. The homogenate was centrifuged at 2,500 rpm at 4 °C for 10 min to pellet cell debris and nuclei and to yield the post-nuclear supernatant. Total membrane protein was obtained by ultracentrifugation of the post-nuclear supernatant at 4 °C, 100,000 × *g* for 1 h. The pellet was resuspended in 50 μl of PBS, and aliquots of this fraction containing 10 μg of protein (according to Bradford assay with bovine serum albumin standard) were resolved by 7.5% SDS-PAGE. After transfer to nitrocellulose, MRP1, P-gp, and actin (control) were detected by Western blot analysis using the anti-MRP1 monoclonal antibody MRPm6 (1:200), anti-P-gp monoclonal antibody C219 (1:500), or anti-actin monoclonal antibody (1:500). MRP1 and P-gp antibodies were from Monosan Antibodies, and the actin antibody was obtained from Sigma.

Cellular pH Measurements—Ratiometric pH-sensitive probes, FITC dextran, and (5-and 6-) carboxyl SNARF1 AM acetate ester were used to determine the pH within the lysosomes and cytosol, respectively. Fluorescence measurements were made using a PerkinElmer Life Sciences LS 50B spectrofluorometer. Intralysosomal pH was determined using a slightly modified procedure of Altan *et al.* (16). Briefly, 10^7 cells were incubated with 5 mg/ml FITC-dextran for 30 min. The cells were then washed four times with RPMI 1640 medium (without phenol red) and incubated in the same medium for 24 h in the cell culture incubator. Cells were transferred to PBS, and the fluorescence emissions at 530 nm were measured at two excitation wavelengths, 490 and 450 nm, respectively. The ratio of emission intensities was determined and converted to pH using the previously referenced standard calibration procedure. Cytosolic pH was determined using a slightly modified procedure of Belhoussine *et al.* (19). Briefly, 10^7 cells were incubated with 4 μM (5-and 6-) carboxyl SNARF1 AM acetate ester for 1 h, washed twice with PBS, and resuspended in PBS prewarmed to 37 °C. Fluorescence emission intensities at 580 and 640 nm were measured at an excitation wavelength of 514 nm. The ratio of the emission intensities at the two emission wavelengths was determined and converted to pH using the referenced methodology.

Quantitative Assessment of Daunorubicin Total Cell Uptake—Cells (10^7) were preincubated with 100 μM BSO for 24 h followed by incubation with daunorubicin (2 μM) for 1 h. Cells were pelleted (1000 rpm, 5 min) and washed twice with ice-cold PBS. The pellet was suspended in 0.75 ml of acetonitrile, vortexed for 10 s, and sonicated for 15 min. The resulting suspension was centrifuged at 13,000 rpm for 10 min, and a 500-μl portion of the supernatant was evaporated to dryness. The residue was analyzed by HPLC following dissolution in 100 μl of mobile phase (30% acetonitrile, 70% 10 mM ammonium acetate, pH 8.2). The HPLC system was comprised of a Waters 600E system controller, 616 pump, 717 plus autosampler and 474 fluorescence detector set at 470-nm excitation and 560-nm emission wavelengths (Waters Corp., MA). A C18 reversed phase X-terra column (Waters Corp.) was used for analysis. Extraction efficiencies for daunorubicin from cells were determined by spiking in known amounts of drug (four in total, representing low, medium, and high concentrations) into blank cell pellets and carrying out the previously described extraction procedure. The extraction efficiency was found to be 48.2 ± 2.7%. This standard curve was linear and was subsequently used to calculate cellular drug accumulation from experimental samples.

IC_{50} Evaluations—Cell sensitivity to daunorubicin was determined using 3-(4,5-dimethylthiazol-2-yl)-2,5-diphenyltetrazolium bromide (MTT) assay as described by Mosmann (20). Briefly, cells were seeded in quadruplicate on 96-well culture plates at a density of 1×10^4 cells/well and were treated with selected concentrations of either daunorubicin or SR101 and then incubated for a period of 3 days. At the end of the incubation period, 10 μl of a 5 mg/ml solution of MTT in PBS was added to each well, and the plates were returned to the incubator for an additional 4 h. A 100-μl portion of Me_2SO was added to each well, and the absorbance was measured at a wavelength of 590 nm in a microplate reader. For SR101, cell viability was determined using trypan blue staining with a hemacytometer since the color of SR101 interfered with the MTT assay. IC_{50} was defined as the concentration of drug causing 50% inhibition of cell growth as compared with untreated control.

RESULTS

Identification of Drug Sequestering Organelles—The model compounds utilized in this study had suitable fluorescence properties that allowed us to visualize their intracellular distribution in cells using a fluorescence microscope. We evalu-

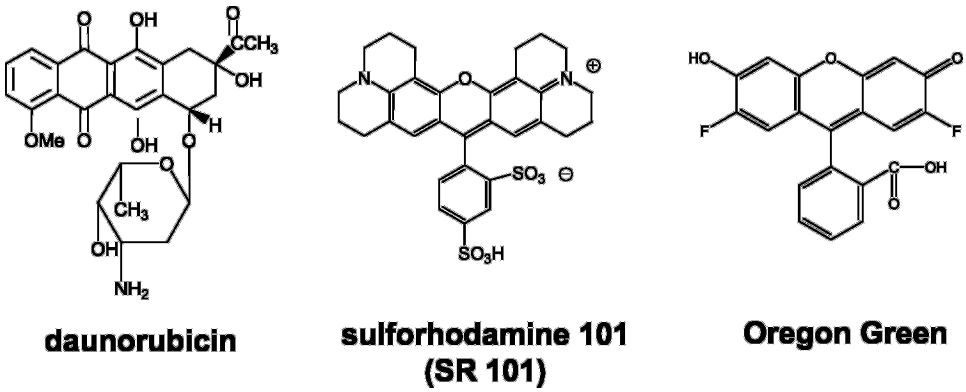

FIG. 1. **Structures of compounds used in this study.** Daunorubicin is a weakly basic anticancer agent. SR101 and Oregon Green are zwitterionic and weakly acidic fluorescent probes, respectively.

ated the intracellular distribution of daunorubicin, SR101, and Oregon Green in the HL-60 ADR cell line and compared this with the parental drug-sensitive cell line using identical incubation conditions. The structures of these three compounds are shown in Fig. 1. Fig. 2 shows that all three compounds displayed somewhat diffuse cellular fluorescence when incubated with drug-sensitive HL-60 cells. In the HL-60 ADR cell line, both daunorubicin and SR101 were sequestered into cytoplasmic organelles; the subcellular distribution of Oregon Green was not significantly altered. In the MDR line, daunorubicin consistently stained cytoplasmic vesicles throughout the cell cytoplasm, whereas SR101 stained a more restricted perinuclear location. This difference prompted us to investigate the identity of drug sequestering organelles. Direct co-localization of daunorubicin and SR101 could not be achieved because of significant overlap of the fluorescent properties for these two molecules. We therefore sought to independently identify drug-sequestering organelles using fluorescence co-localization experiments with organelle-specific fluorescent probes and vital stains. We found that daunorubicin co-localized with the lysosomal vital stain Lysotracker Green (Fig. 3*A*). Considering the fact that lysosomal vital stains such as Lysotracker Green can non-selectively stain additional organelles (21), we further demonstrated the co-localization of daunorubicin with FITC-dextran localized to lysosomes, which is a more specific stain (Fig. 3*B*). The co-localization of daunorubicin with the FITC-dextran further supports the involvement of lysosomes in the sequestration of this compound. Unlike daunorubicin, SR101 was not co-localized with lysosomes (Fig. 4*B*). SR101 was found to co-localize with NBD-C_6 ceramide, a Golgi-specific vital stain (Fig. 4*A*).

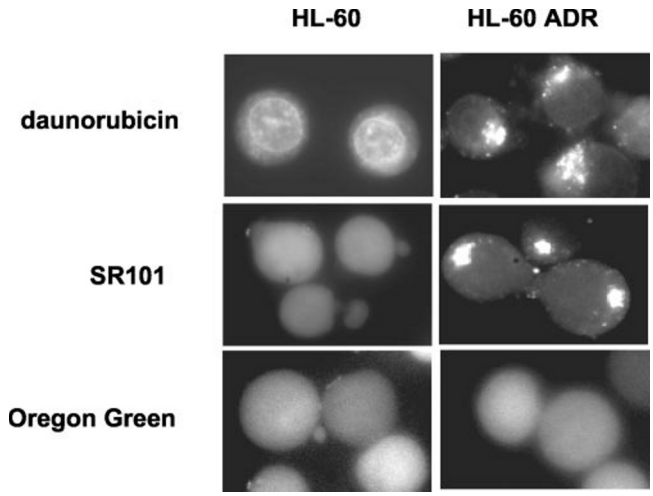

FIG. 2. **Both daunorubicin and SR101 are sequestered into cytoplasmic compartments in the HL-60 ADR cells, a process that does not seem to occur in drug-sensitive cells.** The intracellular distribution of Oregon Green does not change. Cells were incubated with indicated compound for 1 h, washed, and visualized using fluorescence microscopy using appropriate filter sets. The concentrations of compounds used for incubations were 2, 5, and 5 μM for daunorubicin, SR101, and Oregon green, respectively.

Mechanistic Evaluation of Drug Sequestration—We next sought to obtain preliminary results with regard to relevant mechanism(s) for these two compound-sequestering organelles. We first examined the possibility that daunorubicin is sequestered into lysosomes via a pH partitioning mechanism. The theoretical basis for the pH partitioning mechanism requires the lysosome-to-cytosol pH differential to be greater in the MDR line relative to the sensitive line. To test this, we measured the pH of the cytosol and lysosomes for both cell lines. FITC-dextran was used to measure lysosomal pH, and (5-and 6-) carboxyl SNARF1 AM acetate ester was used to measure cytosolic pH. Table I shows that the pH differential is 1.95 in MDR cells but only 0.52 in sensitive cell lines, which is consistent with the pH partitioning mechanism. To further evaluate this, HL-60 ADR cells were preincubated with the proton ionophores nigericin and monensin, which abolish cellular endomembrane pH gradients (18). The distribution of daunorubicin in the HL-60 ADR cells with and without pH gradient disruption is shown in Fig. 5. Cells with disrupted pH gradients were no longer able to sequester daunorubicin into lysosomes, and the cellular distribution now resembled the distribution in drug-sensitive cells. Conversely, the localization of SR101 to the Golgi apparatus was not noticeably affected by pH gradient disruption. Immunofluorescence staining of the lysosomal membrane protein LAMP-1 confirmed that cells with disrupted pH gradients had lysosomal morphology similar to cells without pH disruption (data not shown). This supports the idea that daunorubicin is sequestered into lysosomes by a pH partitioning mechanism, whereas SR101 is sequestered into the Golgi apparatus by an alternative mechanism. For SR101, we anticipated the involvement of drug transporter proteins. We screened for the expression of common drug transporter proteins from whole cell homogenates from sensitive and MDR lines using Western blot analysis (Fig. 6*A*). We found that resistant cells showed a significant overexpression of the drug transporter protein MRP1 in comparison with sensitive cell lines, which had no detectable expression of this protein. We also examined the distribution of the drug transporter P-gp and found no detectable expression in either sensitive or resistant cell lines (data not shown). The intracellular localization of MRP1 in the HL-60 ADR cell was determined using an immunofluorescence protocol. Cells were incubated with a rat monoclonal antibody against MRP1, which was then localized with a

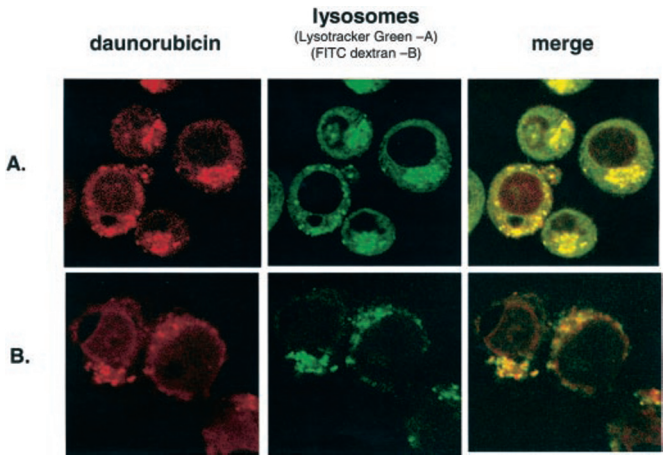

FIG. 3. **Lysosomes are involved in the sequestration of daunorubicin in the HL-60 ADR cell line.** Daunorubicin fluorescence micrographs are shown on the *left panels*. *Middle panels* display the same cells visualizing lysosomes stained with Lysotracker Green (*A*) and with FITC dextran (*B*). *Panels* to the *right* represent the merged images. Daunorubicin incubation conditions are described in the legend for Fig. 2. Lysostracker Green and FITC dextran incubation conditions are described under "Experimental Procedures."

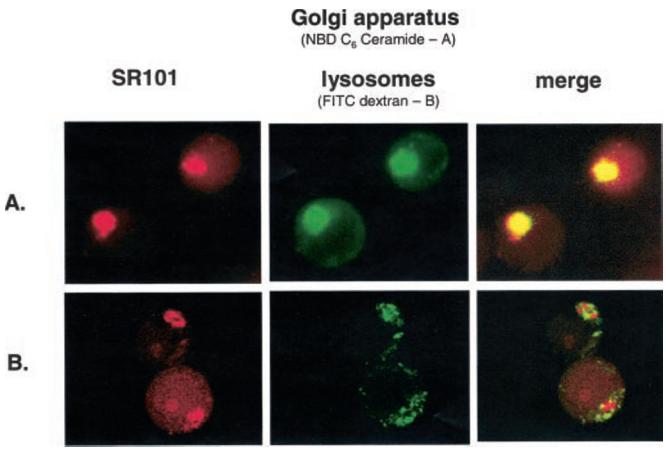

FIG. 4. **SR101 co-localizes with the Golgi apparatus and not with lysosomes in the HL-60 ADR cell line.** The *left column* shows SR101 distribution. The *middle column* shows the fluorescent staining of the Golgi apparatus with NBD-C_6 ceramide (*A*) and of the lysosomes with FITC dextran (*B*). The *right column* is the merge of these two images. SR101 incubation conditions are described in the legend for Fig. 2. NBD-C_6 ceramide incubation conditions are described under "Experimental Procedures."

TABLE I
Experimentally determined lysosomal and cytosolic pH values for HL-60 cells

Values are the means of three determinations ± S.E.

Cell line	Lysosome pH	Cytosol pH	ΔpH[a]
HL-60	6.44 ± 0.17	6.96 ± 0.17	0.52
HL-60 ADR	5.17 ± 0.14	7.12 ± 0.04	1.95
HL-60 ADR + nigericin and monensin[b]	7.4	7.4	0
HL-60 ADR + concanamycin A[c]	7.13 ± 0.11	7.21 ± 0.15	0.08

[a] Represents the lysosome to cytosol pH differential.
[b] Nigericin (10 μM) and monensin (20 μM) were incubated with cells in PBS (pH 7.4) for 30 minutes at 37 °C.
[c] Concanamycin A (20 nM) was incubated with cells for 24 hours at 37 °C prior to pH determinations.

FITC-labeled goat anti-rat secondary antibody (Fig. 6*B*, *lower panel*). This micrograph suggested that MRP1 had a significant degree of intracellular expression in addition to plasma membrane localization. Immunofluorescence staining of the trans-

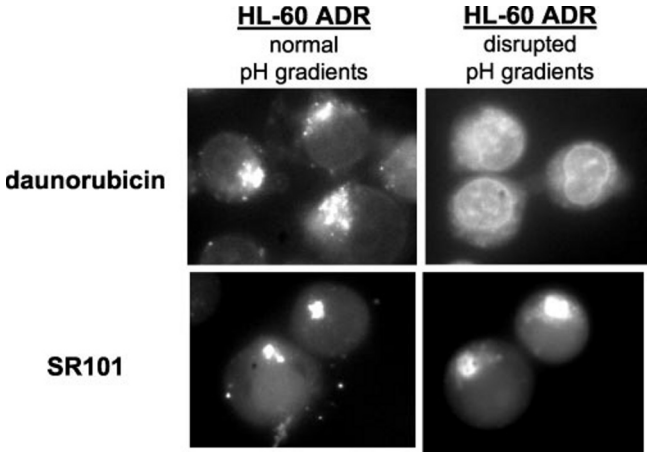

FIG. 5. **Disruption of endomembrane pH gradients leads to release of daunorubicin yet has no effect on the sequestration of SR101 in the HL-60 ADR cell line.** pH gradient disruption was achieved by preincubating cells with nigericin (10 μM) and monensin (20 μM) for 30 min prior to incubation with daunorubicin or SR101 (see the legend for Fig. 2 for conditions).

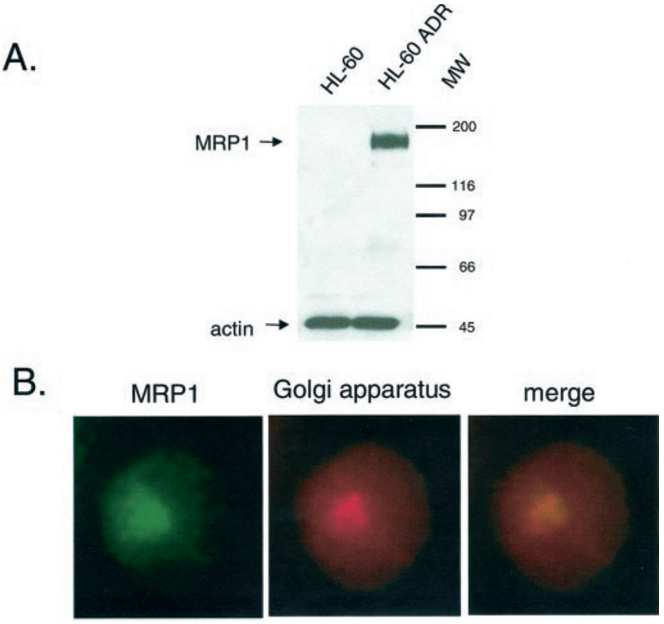

FIG. 6. **HL-60 ADR cells overexpress MRP1, which is localized to the Golgi apparatus.** *A*, Western blot for MRP1 and actin (control) from membrane fractions isolated from HL-60 and HL-60 ADR cell lines. *MW*, molecular weight. *B*, immunofluorescence co-localization of MRP1 and the Golgi-specific protein p230 in the HL-60 ADR cell line. See "Experimental Procedures" for details.

Golgi network with anti-p230 antibody in the same cell is shown in the *middle panel*. The significant overlap of the merged images is consistent with MRP1 presence in the Golgi apparatus. To further demonstrate the role of MRP1 in the sequestration SR101, HL-60 ADR cells were preincubated with the MRP1 inhibitor MK571, and the effect on the intracellular sequestration was evaluated. Fig. 7*A* shows that SR101 fails to be significantly sequestered into the Golgi apparatus in the presence of the MRP1 inhibitor. Contrary to this, the inhibitor had no apparent effect on daunorubicin sequestration. This finding suggests that MRP1 is involved in the sequestration of SR101 in the Golgi apparatus. Moreover, the lack of effect of MK571 on daunorubicin sequestration suggests that daunorubicin sequestration is not mediated by MRP1. MRP1-mediated transport of drugs is often associated with glutathione co-transport or with a covalent coupling of the substrate to gluta-

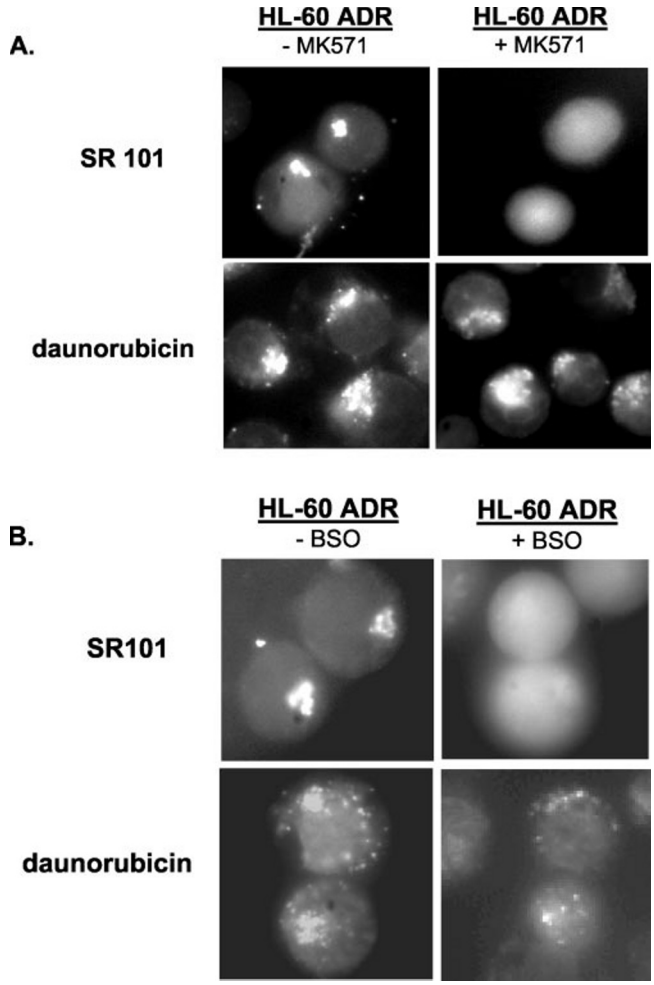

FIG. 7. **The MRP1 inhibitor MK571 and the glutathione-depleting agent BSO disrupt the sequestration of SR101 but have no effect on daunorubicin localization.** In *A*, HL-60 ADR cells were incubated with MK571 (100 μM) for 1 h prior to daunorubicin and SR101 incubation (see the legend for Fig. 2 for conditions). In *B*, HL-60 ADR cells were incubated with BSO (100 μM) for 24 h prior to daunorubicin and SR101 incubation. Note that BSO treatment significantly enhanced daunorubicin accumulation (Fig. 8) and fluorescence intensity. To assess daunorubicin localization patterns, fluorescence gain settings were individually optimized for each of these micrographs.

thione prior to transport (22). Therefore, we evaluated the effect of an inhibitor of cellular glutathione biosyntheses (BSO) on the sequestration of SR101 in the Golgi apparatus. Like MK571, BSO nearly abolished the sequestration capacity of the Golgi apparatus for SR101 yet had no influence on daunorubicin sequestration (Fig. 7*B*). The lack of effect of BSO on daunorubicin sequestration in lysosomes is somewhat surprising since there is evidence that suggests that the activity of vacuolar H+ ATPases may be inhibited by oxidation resulting from glutathione depletion (23, 24). This does not appear to be the case with HL-60 ADR cells under our experimental conditions for BSO treatment. Lysosomal pH was not significantly perturbed (pH values of 5.34 ± 0.08 and 5.15 ± 0.12 in HL-60 ADR cells with and without BSO treatment, respectively). We also did not see any observable change in lysosome morphology with BSO treatment. This was evaluated by comparisons of LAMP-1 immunofluorescence micrographs (data not shown). Nevertheless, this observation is consistent with the requirement of glutathione in the MRP1-mediated transport of SR101 into the Golgi apparatus. HPLC analysis of HL-60 ADR cell extracts revealed only parent SR101; therefore, we think that this step is a glutathione co-transport process rather than a covalent coupling.

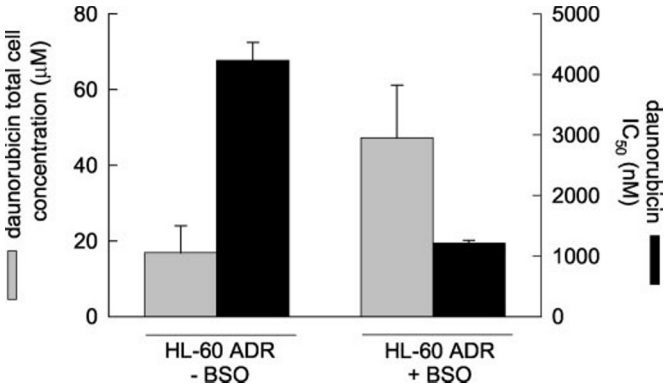

FIG. 8. **Treatment of HL-60 ADR cells with BSO causes an increase in the total cell accumulation of daunorubicin, which results in a corresponding decrease in the daunorubicin IC_{50}.** The *columns* on the *left* are untreated HL-60 ADR cells; those on the *right* have been pretreated with BSO prior to daunorubicin incubation. Data are the means of three experiments ± S.E.

DISCUSSION

In most cases, the intracellular distribution of drugs has been evaluated in cultured cells using fluorescent drugs in conjunction with fluorescence microscopy. The anthracycline antibiotics (*i.e.* daunorubicin, doxorubicin) represent one of the few classes of anticancer agents with suitable fluorescence properties for such analysis. Consequently, most reports studying this drug sequestration phenotype have focused on these weakly basic anticancer drugs. This has led to significant ambiguity regarding the underlying mechanism(s) that drive sequestration because weak bases can be considered likely candidates for drug transporter proteins as well as pH gradient-driven accumulation.

An important consideration that has not been considered previously in the literature is the potential involvement of multiple sequestration mechanisms within a given MDR cancer cell. These mechanisms could function concertedly within a single organelle class, or they could act independently on different organelles. To investigate these possibilities, we evaluated the sequestration capacity for a set of compounds with different acid-base properties: daunorubicin (a weak base chemotherapeutic agent), SR101 (a zwitterionic fluorescent molecule), and Oregon Green (a weakly acidic fluorescent molecule). Of these three molecules, only daunorubicin would be expected to be sequestered into acidic cytoplasmic organelles via a pH-partitioning mechanism. Conversely, considering the broad substrate specificity of drug transporter proteins, all three would be potential candidates for sequestration according to transporter-mediated sequestration mechanism. This approach allowed us to demonstrate that the HL60 ADR cell line has the capacity to sequester different molecules according to different mechanisms into distinct organelles. Our results suggest that SR101 is sequestered into the Golgi apparatus by an MRP1-mediated process, whereas daunorubicin is sequestered into lysosomes according to a pH partitioning mechanism. In both cases, this compartmentalization event can be correlated with increased resistance to the sequestered compound. For daunorubicin, the IC_{50} values in HL-60 and HL-60 ADR cells are 42 ± 5 and 4196 ± 99 nM, respectively; for SR101, these values are 415 ± 94 and 1000 ± 287 μM, respectively. However, both sequestration events correlated with increased resistance, the degree of which appears to be most significant with daunorubicin. This difference can most likely be attributed to different locations and/or mechanisms of cellular toxicity for these two compounds.

Previous mechanistic explanations for daunorubicin sequestration in MDR cell lines have been contradictory. Reports have proposed that a pH partitioning mechanism is responsible (16,

18, 25), yet others have suggested that drug transporters are principally involved (26, 27). The former studies are consistent with our findings in the HL-60 ADR cell line. We have demonstrated the importance of the lysosome-to-cytosol pH gradient in drug sequestration; however, this information alone does not rule out the potential involvement of drug transporter proteins since these proteins could be indirectly participating in drug sequestration through intracellular pH modulation. ATP binding cassette transporters such as P-gp and MRP1 have been shown to influence pH gradients across the plasma membrane of cells (28, 29). Correspondingly, if these transporters are localized to intracellular organelles, it is possible that these transporters could cause acidification of the drug sequestering organelles, if properly oriented. The exact mechanism for reacidification of lysosomes in MDR cells is not known at this time. Normal regulation of organelle pH is carried out by vacuolar (H^+)-ATPases (V-ATPase) and associated ion channels to dissipate membrane potential (30). Our data with HL-60 ADR cells support the idea that lysosomal reacidification in HL-60 ADR cells is regulated by V-ATPase and not by MRP1. In addition, our data suggest that MRP1 is not localized with lysosomes, due to the lack of sequestration of SR101 with daunorubicin in lysosomes (Fig. 4). We have also shown that the specific V-ATPase inhibitor, concanamycin A (Table I), is able to raise lysosomal pH from 5.17 to 7.13 in HL-60 ADR cells, and this resulted in diminished lysosomal sequestration capacity (data not shown), similar to that observed with the proton ionophores shown in Fig. 5. These findings are consistent with those of Ma and Center (31), who have shown that the gene encoding the V-ATPase subunit C is overexpressed in HL-60 ADR cells.

Contrary to our findings, studies have suggested that daunorubicin is sequestered into cytoplasmic organelles of MDR K562 and HL-60 cells according to an MRP1-mediated process (26, 27). Confusion in this identification might be attributed to the inability of the authors to directly co-localize drug transporter with sequestered drug. This is because the permeabilization steps required for immunofluorescence release sequestered compounds. We have circumvented this obstacle by co-localizing MRP1 with the Golgi-associated membrane protein P-230 and separately examining the co-localization of Golgi-specific vital stain NBD-C_6 ceramide with either daunorubicin or SR101. We observed that SR101 was sequestered within the Golgi in HL-60 ADR cells, whereas daunorubicin was not. Studies implicating the involvement of MRP1 in the sequestration of daunorubicin arise from experimental observations using BSO to deplete cellular glutathione. As mentioned earlier, glutathione is thought to be required for the transport of drugs mediated by MRP1. When cells are treated with BSO, previous authors have shown that cells are more sensitive to daunorubicin and that nuclear concentrations of daunorubicin are increased relative to untreated cells (26, 27). However, these studies did not show that BSO was able to directly alter the intracellular sequestration of daunorubicin. Our observations suggest that BSO has no effect on daunorubicin sequestration but indeed mediates the release of SR101 (Fig. 7*B*). We think that the reason for increased nuclear concentrations and increased sensitivity to daunorubicin is due to an increase in total cell accumulation capacity for daunorubicin in BSO-treated cells. To demonstrate this, we quantitatively evaluated daunorubicin sensitivity and total cell accumulation in the HL-60 ADR cell line in the presence or absence of BSO (Fig. 8). In the presence of BSO, we observe an approximately 3-fold increase in whole cell accumulation. We also observe a 3.5-fold increase in sensitivity to daunorubicin, which is in very close agreement with results seen with the 3.1-fold increase observed by Benderra *et al.* (27). As a result, we think that the increase in sensitivity and nuclear accumulation in the presence of BSO is not due to a redistribution of sequestered drug from cytoplasmic organelles, but instead, is directly caused by an overall increase in drug accumulation. Further investigations are required to understand the mechanistic basis for BSO-mediated increase in total cellular accumulation of daunorubicin in this cell line.

In summary, we have shown for the first time that a single MDR cancer cell is capable of sequestering different compounds with different acid/base properties into different organelles. This work demonstrates that the sequestration phenotype associated with certain cancer cells is more complex than originally thought. Many important chemotherapeutic agents are neither weakly basic nor fluorescent. This work may help to rationalize their reduced effectiveness in MDR cancer cells. Furthermore, this information could lead to rational selection/design of new anticancer drugs with a reduced capacity for sequestration. Likewise, specific inhibitors of protein function described in this report may be evaluated as adjuvants in MDR cancer treatment.

REFERENCES

1. Gottesman, M. M., and Pastan, I. (1993) *Annu. Rev. Biochem.* **62,** 385–427
2. Simon, S., Roy, D., and Schindler, M. (1994) *Proc. Natl. Acad. Sci. U. S. A.* **91,** 1128–1132
3. Larsen, A. K., Escargueil, A. E., and Skladanowski, A. (2000) *Pharmacol. Ther.* **85,** 217–229
4. Van der Kokl, D. M., De Vreis, E. G., Muller, M., and Vellenga, E. (2002) *Leuk. Lymphoma* **43,** 685–701
5. Klein, I., Sarkadi, B., and Varadi, A. (1999) *Biochim Biophys Acta* **1461,** 237–262
6. Shapiro, A. B., Fox, K., Lee, P., Yang, Y. D., and Ling, V. (1998) *Int. J. Cancer* **76,** 857–864
7. Meschini, S., Calcabrini, A., Monti, E., Del Bufalo, D., Stringaro, A., Dolfini, E., and Arancia, G. (2000) *Int. J. Cancer* **87,** 615–628
8. Ferrao, P., Sincock, P., Cole, S., and Ashman, L. (2001) *Leuk. Res.* **25,** 395–405
9. Krishnamachary, N., and Center, M. S. (1993) *Cancer Res.* **53,** 3658–3661
10. Van Luyn, M. J., Muller, M., Renes, J., Meijer, C., Scheper, R. J., Nienhuis, E. F., Mulder, N. H., Jansen, P. L., and De Vries, E. G. (1998) *Int. J. Cancer* **76,** 55–62
11. Lage, H., and Deitel, M. (2000) *Lancet Oncol.* **1,** 169–175
12. Sharma, R., Awasthi, Y. C., Yang, Y., Sharma, A., Singhal, S. S., and Awasthi, S. (2003) *Curr. Cancer Drug Targets* **3,** 89–107
13. Martinez-Zaguilan, R., Raghunand, N., Lynch, R. M., Bellamy, W., Martinez, G. M., Rojas, B., Smith, D., Dalton, W. S., and Gillies, R. J. (1999) *Biochem. Pharmacol.* **57,** 1037–1046
14. Skovsgaard, T. (1990) in *Drug Resistance: Mechanisms and Reversal* (Mihich, E., ed) p. 209, John Libbey and Co., New York
15. Moriyama, Y. (1996) *J. Exp. Biol.* **199,** 1447–1454
16. Altan, N., Chen, Y., Schindler, M., and Simon, S. M. (1998) *J. Exp. Med.* **187,** 1583–1598
17. De Duve, C., De Barsy, T., Poole, B., Trouet, A., Tulkens, P., and Van Hoof, F. (1974) *Biochem. Pharmacol.* **23,** 2495–2531
18. Schindler, M., Grabski, S., Hoff, E., and Simon, S. M. (1996) *Biochemistry* **35,** 2811–2817
19. Belhoussine, R., Morjani, H., Millot, J. M., Sharonov, S., and Manfait, M. (1999) *Int. J. Cancer* **81,** 81–89
20. Mosmann, T. (1983) *J. Immunol. Methods. 1983,* **65,** 55–63
21. Haugland RP. (2002) *Handbook of Fluorescent Probes and Research Products* (Gregory, J., ed) 9th Ed., p. 483, Moleuclar Probes, Inc., Eugene, OR
22. Mao, Q., Deeley, R. G., and Cole, S. P. C. (2000) *J. Biol. Chem.* **275,** 34166–34172
23. Forgac, M. (1999) *J. Biol. Chem.* **274,** 1301–1305
24. Oluwatosin, Y. E., and Kane, P. M. (1997) *J. Biol. Chem.* **272,** 28149–28157
25. Hurwitz, S. J., Terashima, M., Mizunuma, N., and Slapak, C. A. (1997) *Blood* **89,** 3745–3754
26. Lutzky, J., Astor, M. B., Taub, R. N., Baker, M. A., Bhalla, K., Gervasoni, J. E., Rosado, M., Stewart, V., Krishna, S., and Hindenburg, A. A. (1989) *Cancer Res.* **49,** 4120–4125
27. Benderra, Z., Trussardi, A., Morjani, H., Villa, A. M., Doglia, S. M., and Manfait, M. (2000) *Eur. J. Cancer* **36,** 428–434
28. Litman, T., Pedersen, S. F., Kramhoft, B., Skovsgaard, T., and Hoffmann, E. K. (1998) *Cell. Physiol. Biochem.* **8,** 138–150
29. Thiebaut, F. T., Currier, S. J., Whitaker, J., Haugland, R. P., Gottesman, M. M., Pastan, I., and Willingham, M. C. (1990) *J. Histochem. Cytochem.* **38,** 685–690
30. Forgac, M. (1999) *J. Biol. Chem.* **274,** 12951–12954
31. Ma, L., and Center, M. S. (1992) *Biochem. Biophys. Res. Commun.* **182,** 675–681